On the timescales in the chaotic dynamics of deterministic systems

P. M. Cincotta

In collaboration with C. M. Giordano

Universidad Nacional de La Plata/Instituto de Astrofísica de La Plata-CONICET, Argentina

Thanks to Carles Simó (UB-Spain) for his valuable comments, suggestions and discussions.

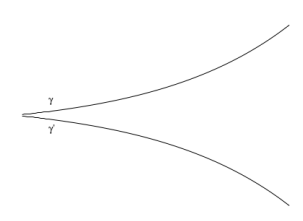
Mar del Plata, April, 2025



Exponential divergence and chaotic diffusion

An specific property of chaotic motion in a non-linear system is the essential sensitivity to initial conditions: orbits starting in an arbitrary small neighborhood U of a given point P of the phase space exhibit an exponential divergence, the maximum Lyapunov exponent at P, σ , is the exponential mean rate.

E.g., if $\delta_0 \equiv |\gamma(0) - \gamma'(0)| \ll 1$ is the initial distance between two nearby trajectories in U, then $\delta(t) \equiv |\gamma(t) - \gamma'(t)| \approx \delta_0 \mathrm{e}^{\sigma t}$.



The evolution of $\delta(t)$ is determined by the first variational equations (or differential map in case of a system of discret time).

- For stable periodic or quasiperiodic motion at P, $\sigma=0$. Locally, the non-linear system is integrable: the full set of local integrals or actions exists.
- The Lyapunov time, $T_L = \sigma^{-1}$, is a microscopical timescale for the hyperbolic dynamics on the tangent space of the phase space at the point P. It is usually assumed to be a characteristic time of predictable dynamics for orbits starting in U.
- ▶ For stable motion $T_L \to \infty$.
- ▶ Chaotic diffusion is a transport process: a statistical description of the chaotic motion of a non-linear system in a macroscopical volume element V around P. Its origin lies in the interaction of resonances and could lead to a macroscopical change in the orbital configuration of the system. e.g. large changes in the prime integrals.
- The timescale for such a change is given by the diffusion time, T_D , or the instability time, $T_{\text{inst.}}$, at V.

Stable chaos

- \blacktriangleright A physical system always has a characteristic lifetime, T_c .
- Exponential divergence of nearby orbits is a necessary but not sufficient condition for chaotic diffusion, stable chaos: the motion could be stable for $T_L \ll T_c < T_{\rm inst}$.
- ▶ The 522 Helga asteroid: it is in a 7/12 resonance with Jupiter, the computed Lyapunov time is $T_L \approx 7 \times 10^3$ yrs however its motion shows stable for timescales larger than $T_{\rm inst} > T_c \sim 10^9$ yrs (Milani & Nobili 1992).
- ▶ The inner Solar System: the orbits of the planets lying in this region exhibit a distribution of the Lyapunov time around $T_L \approx 5 \times 10^6$ yrs though they show stable over a time-scale of the order of $T_{\rm inst} > T_c \sim 10^3 T_L$ (Mogavero et al. 2023).

- Several exoplanet systems exhibit regions of stable chaos and of fast diffusion, i.e. large variation of the shape of the system (Gliese-876 for instance, see Cincotta et al., 2018).
- Stable chaos is associated to a neglectable diffusion speed and it is local, it depends on the position in phase space.
- ► The diffusion speed strongly depends on resonance interactions; invariant manifolds play a crucial role in the existence of stable chaos, while a large overlap of resonances could lead to fast diffusion.
- $ightharpoonup T_{
 m inst}$ is usually determined by direct numerical simulations while T_D is estimated through the diffusion coefficient that characterizes the transport process.
- ▶ In general $T_{\rm inst} \sim T_D$, so it is customary to estimate the instability time through the diffusion time.

Chaos in galaxies

- The presence of chaos in galactic systems was largely discussed in the last fifty years (Contopoulos, Merritt, Pfenniger, Papaphilippou & Laskar among many others).
- ► Realistic galactic models exhibit a large amount of chaotic motion (Maffione et al. 2015, 2018).
- ▶ The early work of Hénon & Heiles (1964), that is the very first report about the numerical evidence of chaotic motion, is in fact a simplified two-dimensional nonlinear axisymmetric galactic potential for the Milky Way.
- ► The aim of that work was to search for the existence of a third integral of motion in the galactic potential.
- ▶ On the other hand, many papers by J. Binney are devoted to the construction of action-angle variables in different galactic potentials; i.e., the Hamiltonian model is assumed integrable or close to it.

Herein we discuss these apparent quite different points of view about the motion of stars in a galaxy.

The galactic model

The model is a frozen potential of an N-body simulation and it is given by a quadrupolar fit with origin at the center of mass (Muzzio et al. 2005, Muzzio 2006):

$$\Phi(\mathbf{r}) = -f_0(\rho_0) - f_x(\rho_x)(x^2 - y^2) - f_z(\rho_z)(z^2 - y^2),$$

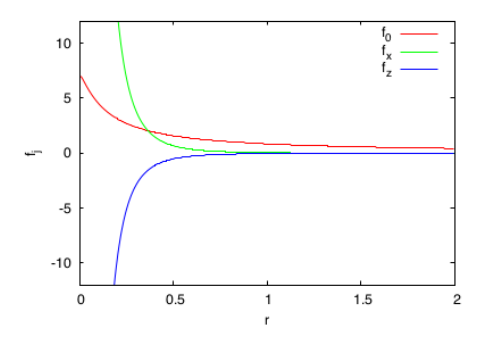
where ρ_j are softening radii defined as

$$\rho_0(r) = \sqrt{r^2 + \epsilon^2}, \quad \rho_x(r) = \rho_z(r) = \sqrt{r^2 + 2\epsilon}, \quad \epsilon = 0.01,$$

and

$$f_j(\rho_j) = \frac{C_j}{\left(\rho_j^{k_j} + q_j^{k_j}\right)^{l_j/k_j}}, \qquad j = 0, x, z.$$

j	C_{j}	k_{j}	q_{j}	l_j
0	0.92012657	1.15	0.1340	1.03766579
\overline{x}	0.08526504	0.97	0.1283	4.61571581
\overline{z}	-0.05871011	1.05	0.1239	4.42030943



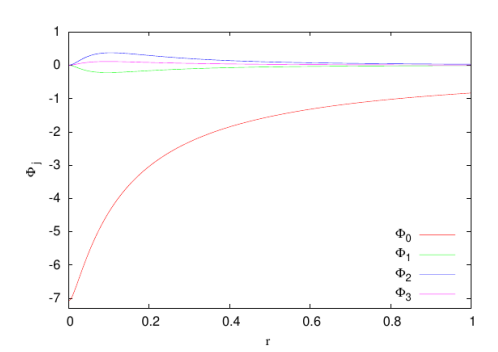
The potential corresponds to a triaxial ellipsoid with semi-axes X,Y,Z satisfying X>Y>Z for any energy label h.

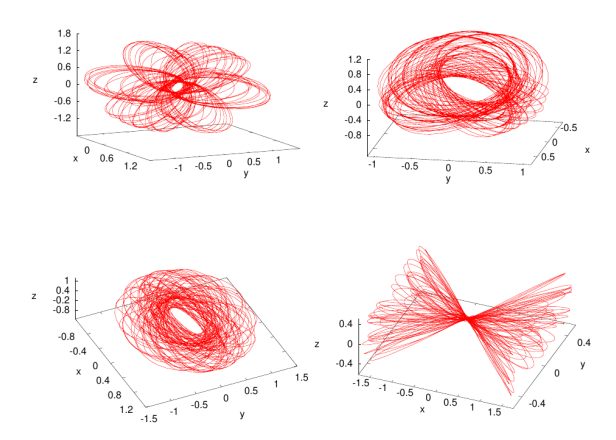
This model reproduces several dynamical properties of elliptical galaxies, such as mass distribution, flattening, triaxiality and so on.

In spherical coordinates (r, θ, ϕ) the potential reads

$$\Phi(r, \theta, \phi) = \Phi_0(r) + \Phi_1(r) \cos 2\phi + \Phi_2(r) \cos 2\theta + \Phi_3(r) (\cos 2(\theta + \phi) + \cos 2(\theta - \phi))$$

where $\Phi_0(r), \Phi_1(r) < 0, \Phi_2(r), \Phi_3(r) > 0$ and when $r \to 0$, all of them vanish but $\Phi_0(0) = \Phi(0)$.

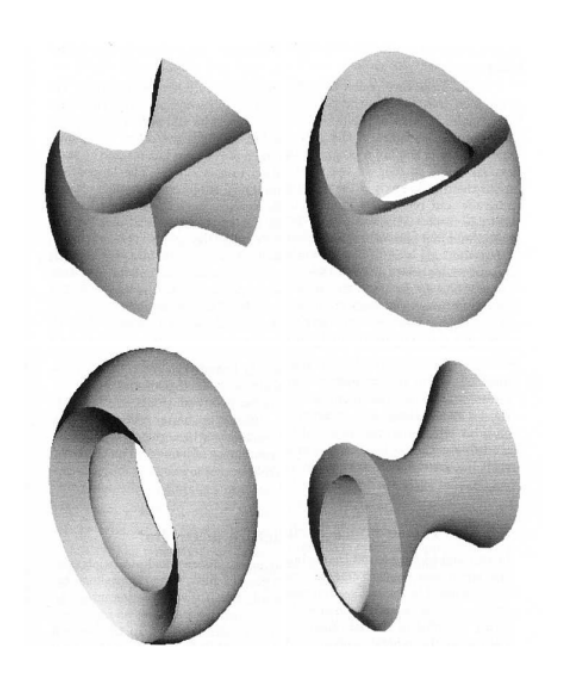




Typical regular (quasiperiodic) orbits in the potential:

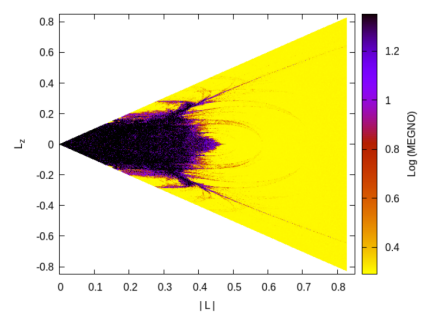
Top: Circulating orbits around the long-axis: outer and inner long-axis tube (left and right).

Bottom: Minor-axis tube at left and at right, a box orbit that oscillates along the long-axis.



Tube orbits (circulating orbits)

Since $|\Phi_j|/|\Phi_0| \ll 1$, j=1,2,3, we assume $|\boldsymbol{L}|$, L_z as unperturbed integrals and setting $x_0=z_0=0,y_0=0.9,h\!=\!-0.5$, $(L_y=0)$, the L space samples the circulating orbits.



MEGNO contour plot in the $(|L|, L_z)$ space. Bright yellow denotes stable motion while violet and black correspond to chaotic and strong chaotic motion.

- ► The short-axis tube orbits lie in the narrow strips bounded by the separatrix at $L_z \sim \pm L$.
- The inner and outer long-axis tubes are separated by the pendulum like separatrix that cross $L_z=0$ near $L\approx 0.60$.
- ightharpoonup The outer long-axis tubes appear at large L.

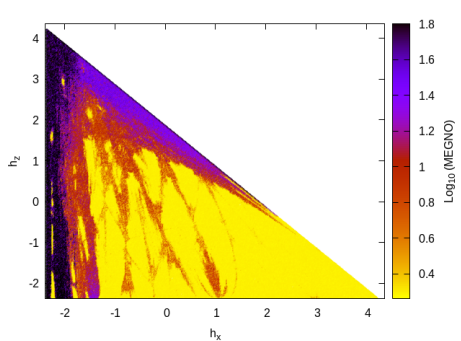


Box orbits

Since oscillating orbits cross the origin, we adopt the energies h_x and h_z as unperturbed integrals restricted to (x,y,z)=(0,0,0):

$$h_x = \frac{p_x^2}{2} + \frac{a_0}{3}, \quad h_z = \frac{p_z^2}{2} + \frac{a_0}{3}, \quad a_0 = \Phi_0(0) \approx -7.084,$$

 $h_y = h - h_x - h_z$ and thus the h space samples oscillating orbits.



MEGNO contour plot in energy space for h=-0.5.

The axial periodic orbits appear at each corner.

Diffusion

The MEGNO contour plots in L and h spaces provide a measure of the maximum Lyapunov exponent and thus of T_L in each point. What about diffusion and T_D ?

- Take small ensembles of $n_p=500$ random initial values of $(|\boldsymbol{L}|,L_z)$ at $x_0=0,y_0=0.9,z_0=0$ and (h_x,h_z) at $x_0=y_0=z_0=0$.
- ▶ Introduce the sections or slices: $S_L : |x| + |y 0.9| + |z| < 0.01$, $S_h : |x| + |y| + |z| < 0.01$.
- ▶ Integrate each of the n_p initial conditions up to 1.5×10^5 time units and look for the intersections of the orbits with S_L and S_h .
- lacktriangle Since we adopted h_x,h_z on the origin as unperturbed integrals in energy space, the potential is expanded in powers of the coordinates such that

$$\Phi(\mathbf{r}) = a_0 + a_1 x^2 + a_2 y^2 + a_3 z^2 + \mathcal{O}(x^3, y^3, z^3),$$

where

$$a_0 = -7.0842, a_1 = 1113.051, a_2 = 2027.408, a_3 = 2166.527.$$

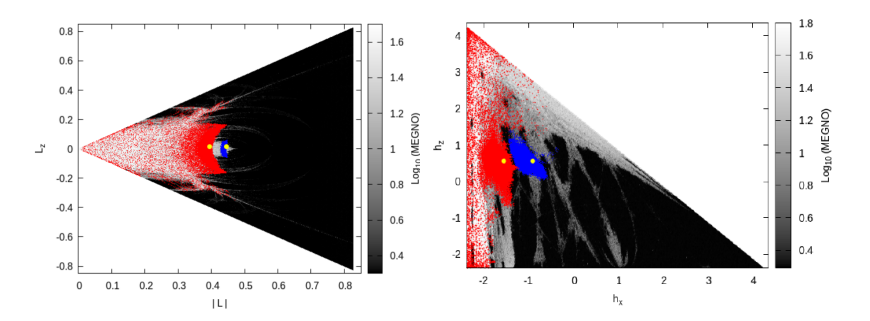
Thus, on the section $S_h: |x| + |y| + |z| < 0.01$, the energies reduce to

$$h_x = \frac{p_x^2}{2} + \frac{a_0}{3} + a_1 x^2, \quad h_z = \frac{p_z^2}{2} + \frac{a_0}{3} + a_3 z^2,$$

where (p_i, x_i) are the actual numerical values corresponding to the motion in the full potential.

On
$$S_h$$
, $a_j x_j^2 < 0.2 \ll |a_0/3|$, $j = 1, 2, 3$.

Examples



Diffusion of two initial ensembles (indicated as a yellow point) in blue and red, for $t \leq 1.5 \times 10^5$, onto a gray scale MEGNO contour plot in L and h spaces.

The diffusion coefficient

Define

 $J^2 = |\boldsymbol{L}|^2 + L_z^2$ in angular momentum space,

 $I^2 = h_x^2 + h_z^2$ in energy space,

a fast action or integral. Denote with y either J or I.

In the normal diffusion approximation the variance of the action values scales with time as

$$var(y(t)) = 4D_y t$$
, (eventually + a constant),

where D_y is the diffusion coefficient at the center of the ensemble.

In the anomalous regime, a power law with time is expected,

$$var(y(t)) = 4\hat{D}_y t^b,$$

 \hat{D}_y being a diffusion-like coefficient, its physical dimensions depends on the Hurst exponent b.

Two variances can be defined after a motion time T:

The *ensemble variance* (not restricted to any section S):

$$var(y(t)) = \frac{1}{n_p} \sum_{i=1}^{n_p} (y(t) - y(0))^2, \quad t \le T.$$

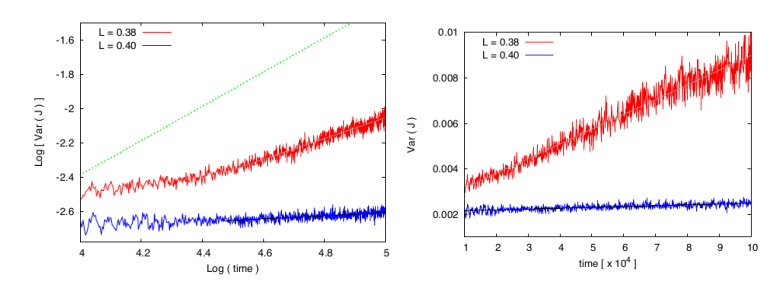
The variance over the section S:

take a fixed interval $\Delta t \ll T$, let $t_l = l\Delta t$ and consider motion times $t_{l-1} < t \le t_l, \ l \in \mathbb{Z}$. Let $n_l \gg 1$ be the intersection of the n_p initial trajectories with $\mathcal S$ at times $\tau_l \in (t_{l-1}, t_l]$, thus the variance over the section is defined as

$$\operatorname{var}(y(t_l)) = \frac{1}{n_l} \sum_{k=1}^{n_l} \left(y^{(k)}(\tau_l) - y^{(k)}(0) \right)^2.$$

In general both variances evolve with the same diffusion rate.

Angular momentum space



Left: The ensemble variance $\mathrm{var}(J)$ vs. time in logarithmic scale. The lines correspond to the least-squares fits of a power law in the interval $3\times 10^4 \le t \le 10^5$ while the green doted one to a line of unitary slope. **Right:** Similar to the left but in linear scale and fitting a normal law.

Anomalous: $b \approx 0.61, \ b \approx 0.09; \ \hat{D}_J \approx 4 \times 10^{-6}, \ \hat{D}_J \approx 4.4 \times 10^{-4}.$

Normal: $D_J \approx 3.2 \times 10^{-8}$, $D_J \approx 1.8 \times 10^{-9}$.

In any case, the errors are less than 7%.



These results are in some sense confusing, since it is not possible to decide if the diffusion is normal or not, and moreover, what is the value of the diffusion time?

In the case of the normal assumption, the diffusion time, from $\mathrm{var}(J)=4Dt=\Lambda^2,$ is

$$T_D = \frac{\Lambda^2}{4D_J},$$

where Λ^2 is some mean square displacement in L space.

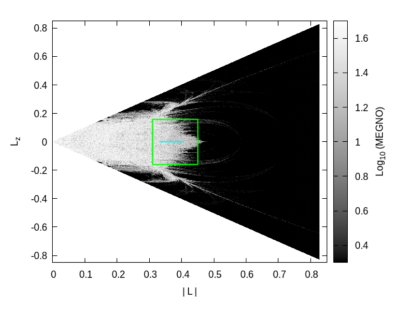
Similarly, in the anomalous scenario it is

$$T_{\hat{D}} = \left(\frac{\Lambda^2}{4\hat{D}_J}\right)^{1/b}.$$

It is simple to check that both time-scales could differ in several orders of magnitude. For instance, setting $\Lambda^2 = 0.25$, in the case of $|\mathbf{L}| = 0.40$,

$$T_D \approx 3.5 \times 10^7$$
, $T_{\hat{D}} \approx 8.3 \times 10^{23}$.

The instability time



Define the instability time, $T_{\rm inst}$, as the required motion time for the orbits starting at initial ensembles on the segment at $0.33 \leq |\boldsymbol{L}| < 0.404$, $L_z = 10^{-4}$ to cross any of the boundaries shown in figure on the section \mathcal{S}_L . The motion time considered is $T = 1.5 \times 10^5$, so $T_{\rm inst} \leq T$.

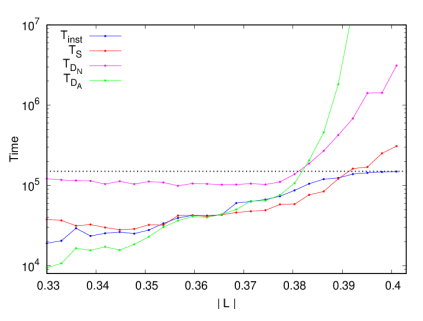
In order to reduce stickiness effects, the diffusion time is defined as the average value over the n_p initial conditions in the ensemble.

By recourse of the Shannon entropy, a diffusion coefficient D_S can be derived and it provides accurate estimates of the instability time (Cincotta et al, 2021, 2022, 2023).

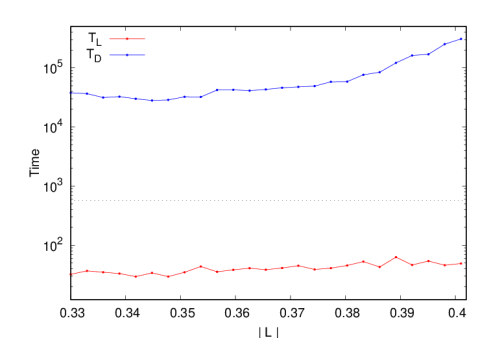
For all these ensembles we also compute D_J and \hat{D}_J, b and after setting $\Lambda=0.07$ (half of the length of the rectangle), we estimate

$$T_D = \frac{\Lambda^2}{4D_J}, \quad T_{\hat{D}} = \left(\frac{\Lambda^2}{4\hat{D}_J}\right)^{1/b}, \quad T_S = \frac{\Lambda^2}{4D_S}$$

and compare these estimates with $T_{\rm inst}$.



For the same ensembles we compute the Lyapunov time, T_L , as the average over the n_p initial conditions and adopting T_S as an estimate of the instability time or diffusion time we get



- ▶ A lifetime for a galaxy is \sim the Hubble time, $T_H \approx 1.4 \times 10^{10}$ yrs.
- ▶ In galactic dynamics T_H is given in terms of the so-called crossing time, typically, $T_{\rm cross} \sim 10^8$ yrs and in general, $T_H \lesssim 500 T_{\rm cross}$.
- ▶ In this model, $T_{\rm cross} \approx 0.575$ time units, thus an upper bound to T_H is $T_c = 1000 T_{\rm cross} = 575$. The dotted line in the figure denotes this value and clearly $T_L \ll T_c \ll T_D$: stable chaos.

The energy space

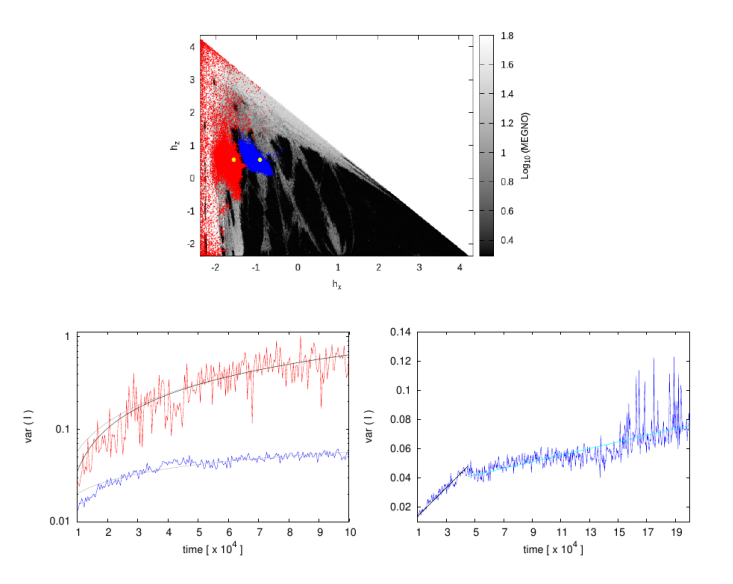
In this model, the average amount of chaos in the h space is about 65% while in the L space it reduces to about 15%. Thus it would be expected that the diffusion could lead to larger changes in the integrals in physical times.

The results concerning the variance approach are similar to those shown for the L space, but now we deal with the *variance over the section*, since the unperturbed integrals h_x, h_y, h_z are defined on the section $\mathcal{S}_h: |x|+|y|+|z|<0.01$:

$$h_x = \frac{p_x^2}{2} + \frac{a_0}{3} + a_1 x^2, \quad h_z = \frac{p_z^2}{2} + \frac{a_0}{3} + a_3 z^2,$$

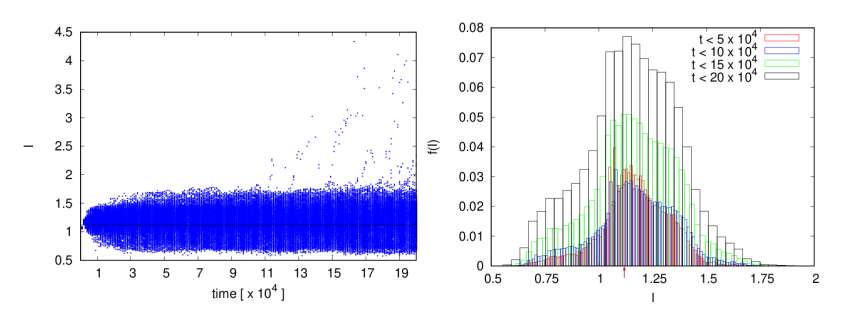
and

$$I^2 = h_x^2 + h_z^2.$$



Anomalous : $b \approx 1.04$, $b \approx 0.45$; $\hat{D}_I \approx 10^{-6}$, $\hat{D}_I \approx 7.6 \times 10^{-5}$. Normal : $D_I \approx 1.7 \times 10^{-6}$, $D_{I1} \approx 2.4 \times 10^{-7}$, $D_{I2} \approx 5.7 \times 10^{-8}$.

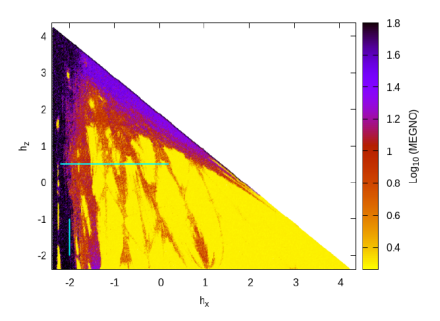
Evolution and distribution of ${\cal I}$ for the ensemble showing anomalous diffusion:



The average is almost constant: 1.176, quite close to the location of the initial ensemble, while the standard deviation slowly increases with time: 0.155, 0.186, 0.201, 0.217 for $t \leq 5 \times 10^4, \leq 10^5, \leq 1.5 \times 10^5, \leq 2 \times 10^5$ respectively.

The departure from a normal distribution explains the anomalous diffusion observed.

The instability or diffusion time



For ensembles on both segments, instead of deriving the instability time by plain numerical simulations, an upper bound for the variation of the energies over a physical meaningful time-scale can be derived.

Setting $T_{\rm inst}=T_c=1000T_{\rm cross}=575$, and since $T_{\rm inst}=\Lambda^2/4D_S$ we obtain an upper bound for the change in the energies,

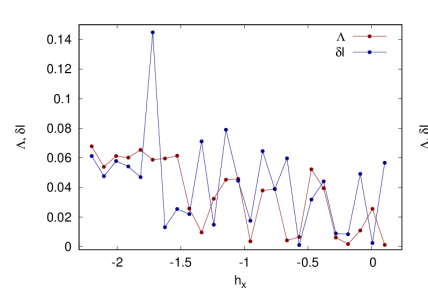
$$\Lambda \approx 48\sqrt{D_S}$$
.

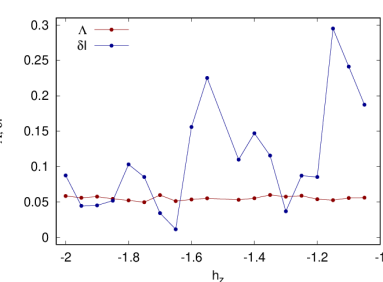
For comparison we also compute an independent estimate of changes in I. Let $\{I_1, I_2, \ldots, I_N\}$ be the values of the fast action on \mathcal{S}_h for the n_p trajectories after $t \leq T_c$, then the variation of I is computed as

$$\delta I^2 = \frac{1}{N} \sum_{i=1}^{N} (I_i - I(0))^2,$$

where I(0) is the central value of the ensemble.

After removing those ensembles located in stable regions we obtain





- ▶ In any case, over a time-scale $T_c = 575 > T_H$, the changes in the integrals are quite small, $\Lambda < 0.07$.
- ▶ The Lyapunov times are in the interval $23 < T_L < 34$ for the vertical segment and $25 \le T_L < 250$ for the horizontal one (removing the stable cases).
- ▶ Therefore macroscopical changes in the integrals could only occur for diffusion times satisfying $T_L < T_c \ll T_D$: stable chaos.

Final remarks

- Regarding the model, the adopted potential corresponds to an isolated elliptical galaxy.
- In this model, even in the most chaotic regions of the phase space, we found stable chaos, $T_L < T_c \ll T_{\rm inst}$.
- ► This result seems to be global, it applies for any energy value and position in phase space.
- Since physical time scales are bounded by $\sim 400T_{\rm cross}$, motion times of this order could be large enough to reveal the exponential divergence of nearby orbits yielding a relatively small T_L , but too short for the transport process to operate, i.e., macroscopical instabilities would be completely irrelevant.
- ▶ Therefore T_L is, in fact, a lower bound to predictable dynamics since a timescale for a macroscopical instability is $T_D \sim T_{\rm inst} \gg T_L$.
- ▶ Similar results were found for a 4D symplectic map (Cincotta & Giordano 2024) where we conjecture that stable chaos is expected to be dominant in almost all predictable dynamical systems, except for those that could be regarded as nearly ergodic.

Regarding the results for galaxies

- All this may change since galaxies are not isolated.
- Perturbations such as interactions with nearby galaxies (at the present or in the past) should be considered and could lead to a different dynamics.
- Moreover we are neglecting the role of gas physics (at the present or in the past) that could play a relevant role in the kinematics of a galaxy.
- ▶ Recent results from a Galaxy Survey (SAMI) reveal that those galaxies that exhibit thermal (chaotic) motion are much older than those where the motion is mostly ordered (Croom et al. 2024).
- ▶ Maybe a more realistic model, including galaxy interaction and gas could lead to a faster diffusion and thus smaller diffusion times, but the results presented herein are, in some sense, in agreement with this study, the age of a galaxy is crucial for the existence of macroscopical changes in the orbital configuration.

Some references

- B. V. Chirikov, A universal instability of many-dimensional oscillator systems, Phys. Rep., 52, 263 (1979) as well
 as many of his articles, available at https://www.quantware.ups-tlse.fr/chirikov/publclass.html
- A. Milani, A. M. Nobili, An example of stable chaos in the Solar System, Nat. 357, 569 (1992).
- F. Mogavero, N. H. Hoang, J. Laskar, Timescales of chaos in the inner Solar System: Lyapunov spectrum and quasi-integrals of motion, Phys. Rev. X, 13, 021018 (2023).
- P. M. Cincotta, C. M. Giordano, C. Beaugé, J. Martí, On the chaotic diffusion in multidimensional Hamiltonian systems, Celest. Mech. and Dyn. Astron., 130, article id. 7, 23. (2018)
- M. Hénon, C. Heiles, The Applicability of the Third Integral Of Motion: Some Numerical Experiments, Astronon. Jour., 69, 73 (1964)
- G. Contopoulos G., Order and Chaos in Dynamical Astronomy, Springer-Verlag, Berlin (2002)
- D. Merritt, T. Fridman, Triaxial Galaxies with Cusps, Astrophys. Jour., 460, 136 (1996)
- D. Merritt, M. Valluri, Chaos and Mixing in Triaxial Stellar Systems, Astrophys. Jour, 471, 82 (1996)
- Y. Papaphilippou, J. Laskar, Global dynamics of triaxial galactic models through frequency map analysis, Astron. Astrophs., 329, 451 (1998)
- N. Maffione et al, On the relevance of chaos for halo stars in the solar neighbourhood I, II Mon. Not. R. Astron. Soc., 453, 2830 (2015); 478, 4052 (2018)
- J. Binney, Orbital tori for non-axisymmetric galaxies, Mon. Not. R. Astron. Soc., 474, 2706 (2018)
- J. C. Muzzio, D. D. Carpintero, F. C. Wachlin, Spatial Structure of Regular and Chaotic Orbits in a Self-Consistent Triaxial Stellar System, Celest. Mech. Dyn. Astron., 91, 173 (2005)
- J. C. Muzzio, Regular and chaotic orbits in a self-consistent triaxial stellar system with slow figure rotation, Celest. Mech. Dyn. Astron., 96, 85 (2006)
- P. M. Cincotta, I.I. Shevchenko, Correlations in area preserving maps: A Shannon entropy approach, Physica D, 402, 132235 (2020)
- P. M. Cincotta, C. M. Giordano, R. Alves Silva, C. Beaugé, The Shannon entropy: An efficient indicator of dynamical stability, Physica D., 417, 132816 (2021)
- P. M. Cincotta, C. M. Giordano, R. Alves Šilva, C. Beuagé, Shannon entropy diffusion estimates: sensitivity on the parameters of the method, Celest. Mech. Dyn. Aston., 133, 7 (2021)
- P. M. Cincotta, C. M. Giordano, Estimation of diffusion time with the Shannon entropy approach, Phys. Rev. E., 107, 064101 (2023).
- P. M. Cincotta, C. M. Giordano, Chaotic diffusion in a triaxial galactic model: an example of global stable chaos, Russian Journal of Nonlinear Dynamics, DOI: 10.20537/nd240801 (2024)
- S. M. Croom, et al., The SAMI Galaxy Survey: galaxy spin is more strongly correlated with stellar population age than mass or environment, Mon. Not. R. Astron. Soc. 529, 3446 (2024)
- P. M. Cincotta, C. M. Giordano, On the time-scales in chaotic dynamics, Chaos, 34, 103109 (2024)

The entropy approach (improved) - Extra material

Let us consider a dynamical system specified by $q\gg 1$ different states, the probability of being in a given state depending on a parameter p. Let $\mu_p^{(k)}(t),\ k=1,\ldots,q$ be the probability of the system to be in the k-th state at time t. The Shannon entropy is defined as

$$S_p(t) = -\sum_{k=1}^{q} \mu_p^{(k)}(t) \ln(\mu_p^{(k)}(t)), \qquad \mu_p^{(k)} \neq 0,$$

while $S_p(t) = 0$ whenever $\mu_p^{(k)} = 0$, $\forall k$.

If for a given p, the system is confined just to the l-th state for all t, then $\mu_p^{(k)} = \delta_{lk}$ and $S_p = 0$, its minimum value. In this case $\dot{S}_p = 0, \ \forall t.$

If for some p, and t large enough, all the $\mu_p^{(k)}$ are equal, then the system has the same probability of being in any of the q states, $\mu_p^{(k)}=1/q$. The entropy then takes its maximum value, $S_p=\ln q$.

Let us focus on the evolution of the entropy and assume that for a given p, the system behaves as a nearly random one. Thus for t>0 but not too large, the system could be in $r_p(t)\ll q$ states, all of them with nearly the same probability. Then $S_p(t)\approx \ln r_p(t)$ and

$$\dot{S}_p \approx \frac{\dot{r}_p(t)}{r_p(t)} > 0,$$

the time derivative of the entropy rates the increase of the number of states the system transits through, $\dot{r}_{p}(t)$.

Identify the parameter p with a given initial point in the h or L space (y_1,y_2) , and the different states with q small 2-dimensional cells covering all possible values of the integrals in the finite domain $\Delta y_1 \Delta y_2$. The size of each cell is then taken as

$$\delta_q = \frac{\Delta y_1 \Delta y_2}{q},$$

At t=0 the system is in a single cell, that corresponding to the initial values of (y_1,y_2) on the section \mathcal{S} , but for t>0 the diffusion carries y_1 and y_2 over different cells. Thus after a motion time t we can heuristically relate r(t) with the mean square displacement of the actions, $L^2(t)$,

$$\delta_q r(t) \approx 2L^2(t),$$
 (1)

and the evolution of r(t) is determined by the transport process in action plane. This assumption appears in all previous formulation of the entropy approach. Let us discuss it.

In the normal diffusion approximation, the distribution function of the actions $\rho(y_1,y_2,t)$ with $-\infty < y_1,y_2 < \infty$, satisfies a diffusion equation of the form

$$\frac{\partial \rho}{\partial t} = D_1 \frac{\partial^2 \rho}{\partial y_1^2} + D_2 \frac{\partial^2 \rho}{\partial y_2^2},$$

where D_i is the corresponding diffusion coefficient.

At t=0 all action values in an ensemble are nearly the same, then

$$\rho(y_1, y_2, 0) = \delta(y_1 - y_1(0))\delta(y_2 - y_2(0)).$$

The solution, $\rho(y_1,y_2,t)$, is a normal distribution with mean $\langle y_1 \rangle = y_1(0)$, $\langle y_2 \rangle = y_2(0)$ and the variance satisfying

$$var(y_1) = 2D_1t$$
, $var(y_2) = 2D_2t$.

Let us compute r(t) for a normal diffusion process. Being

$$\rho(y_1, y_2; \sigma_1(t), \sigma_2(t)) = \rho_1(y_1; \sigma_1(t)) \rho_2(y_2, \sigma_2(t))$$

the distribution of the actions at time t and since the mean value is irrelevant, we assume that the diffusion spreads out from the origin. The cell size δ_q can be splitted in each direction as

$$\delta_1 \times \delta_2 = \frac{\Delta y_1}{q_1} \times \frac{\Delta y_2}{q_2},$$

with $q_1q_2=q$ and $q_1,q_2\gg 1$, and since Δy_j is finite and not too large, it follows that $\delta_1,\delta_2\ll 1$.

Let $(y_{1k}, y_{2l}) = (k\delta_1, l\delta_2)$ be the center of the kl-th cell,

$$k = -[q_1/2], \dots, [q_1/2], l = -[q_2/2], \dots, [q_2/2],$$
 []: integer part.

Then the measure of the kl-th cell, a_{kl} , is

$$\begin{split} \mu(a_{kl}) &= & \int_{a_{kl}} \rho_1(y_1;\sigma_1) \rho_2(y_2;\sigma_2) dy_1 dy_2 \\ &= & \int_{y_{1(k-1)}}^{y_{1k}} \rho_1(y_1;\sigma_1) dy_1 \int_{y_{2(l-1)}}^{y_{2l}} \rho_2(y_2;\sigma_2) dy_2. \end{split}$$

The above integrals would provide a non-negligible value of $\mu(a_{kl})$ whenever

$$|y_{1k}| \le s_1 \sigma_1, |y_{2l}| \le s_2 \sigma_2, \quad s_1, s_2 \sim 1,$$

SO

$$|k| \leq \left[\frac{s_1\sigma_1}{\delta_1}\right] = \left[\frac{s_1\sigma_1}{\Delta y_1}q_1\right] \leq \left[\frac{q_1}{2}\right], \ |l| \leq \left[\frac{s_2\sigma_2}{\delta_2}\right] = \left[\frac{s_2\sigma_2}{\Delta y_2}q_2\right] \leq \left[\frac{q_2}{2}\right].$$

Therefore the (maximum) number of cells visited by the motion would be $r \approx 2k2l$

$$r\approx 4s_1s_2\frac{\sigma_1\sigma_2}{\delta_1\delta_2},\quad \rightarrow \quad \delta_q r\approx 4\sigma_1\sigma_2,$$

after setting $s_1 \approx s_2 \approx 1$. Notice that r depends on the product of the standard deviations in each degree of freedom.

Since
$$\sigma_j = \sqrt{\operatorname{var}(y_j)} = \sqrt{2D_j t}, \ j = 1, 2$$

then

$$\delta_q r(t) \approx 8 \sqrt{D_1 D_2} t = 8 \bar{D} t, \qquad \bar{D} = \sqrt{D_1 D_2}.$$

In the case of the heuristical conjecture, $\delta_q r(t) \approx 2L^2(t)$, setting $L^2(t) \approx \sigma_1^2(t) + \sigma_2^2(t)$, it leads to

$$\delta_q r(t) \approx 4(D_1 + D_2)t = 8\langle D \rangle t, \qquad \langle D \rangle = \frac{D_1 + D_2}{2}.$$

For isotropic diffusion, $D_1=D_2=D$, $\delta_q r(t)\approx 8Dt$ and the entropy $S\approx \ln r$ evolves logarithmically with Dt and we can define

$$D_S \approx \frac{1}{8} \delta_q \frac{r}{t} \approx \frac{\delta_q}{8t} e^S.$$

When the transport is not normal over the full time-span, the diffusion coefficient can be defined just in the interval (t,t+dt). Thus a local entropy-like diffusion coefficient is defined as

$$D_S(t) := \frac{1}{8} \delta_q \frac{dr}{dt}.$$

Since $\dot{r}(t) \approx r(t) \dot{S}(t)$, D_S can be recast as

$$D_S(t) = \frac{1}{8}\delta_q r(t) \frac{dS}{dt}.$$

Thus defined, $D_S(t)$ has the right physical dimensions and should be independent of time for large enough t.

If we take some finite small time-step Δt , the motion time interval (0,t) can be divided in small sub-intervals $j\Delta t, j=1,\ldots,n$ where the diffusion coefficient in each j-th interval, $D_S(t_j)$, is given by the local diffusion coefficient $D_S(t)$.

In general since the transport is neither isotropic, homogeneous nor time-independent, an average procedure to numerically estimate D_S after a motion time t follows

$$D_S = \frac{1}{n - j_0} \sum_{j=j_0}^{n} D_S(t_j),$$

where $j_0 > 1$ is introduced in order to avoid any initial transient.

In order to justify that indeed $S \approx \ln r, \, r < q$, consider $N \gg 1$ values of y_1 and y_2 and let n_k those falling within the k < q cell, then the entropy

$$S = -\sum_{k=1}^{q} \mu_k \ln \mu_k = \ln N - \frac{1}{N} \sum_{k=1}^{r} n_k \ln n_k.$$

According to Cincotta and Shevchenko (2020), assuming that n_k follows a Poisson distribution with mean value $\lambda=N/r\gg 1$ then,

$$S \approx \ln r + \mathcal{O}(\lambda^{-1}).$$